International Journal of Geo-Information

MDPI

Article

Feasibility of Emergency Flood Traffic Road Damage Assessment by Integrating Remote Sensing Images and Social Media Information

Hong Zhu [1], Jian Meng [2,3,*], Jiaqi Yao [4,5] and Nan Xu [6]

[1] College of Ecology and Environment, Institute of Disaster Prevention, Beijing 101601, China; zhong@cidp.edu.cn
[2] School of Earth Sciences and Engineering, Institute of Disaster Prevention, Beijing 101601, China
[3] Beijing Disaster Prevention Science and Technology, Co., Ltd., Beijing 101100, China
[4] Hebei Key Laboratory of Resource and Environmental Disaster Mechanism and Risk Monitoring, Sanhe 065201, China; 201981020027@sdust.edu.cn
[5] Academy of Eco-Civilization Development for Jing-Jin-Ji Megalopolis, Tianjin Normal University, Tianjin 300387, China
[6] College of Geography and Remote Sensing, Hohai University, Nanjing 210024, China; hhuxunan@hhu.edu.cn
* Correspondence: mengjian@cidp.edu.cn

check for updates

Citation: Zhu, H.; Meng, J.; Yao, J.; Xu, N. Feasibility of Emergency Flood Traffic Road Damage Assessment by Integrating Remote Sensing Images and Social Media Information. *ISPRS Int. J. Geo-Inf.* **2024**, *13*, 369. https://doi.org/10.3390/ijgi13100369

Academic Editors: Godwin Yeboah and Wolfgang Kainz

Received: 12 August 2024
Revised: 12 October 2024
Accepted: 16 October 2024
Published: 18 October 2024

Correction Statement: This article has been republished with a minor change. The change does not affect the scientific content of the article and further details are available within the backmatter of the website version of this article.

Copyright: © 2024 by the authors. Published by MDPI on behalf of the International Society for Photogrammetry and Remote Sensing. Licensee MDPI, Basel, Switzerland. This article is an open access article distributed under the terms and conditions of the Creative Commons Attribution (CC BY) license (https://creativecommons.org/licenses/by/4.0/).

Abstract: In the context of global climate change, the frequency of sudden natural disasters is increasing. Assessing traffic road damage post-disaster is crucial for emergency decision-making and disaster management. Traditional ground observation methods for evaluating traffic road damage are limited by the timeliness and coverage of data updates. Relying solely on these methods does not adequately support rapid assessment and emergency management during extreme natural disasters. Social media, a major source of big data, can effectively address these limitations by providing more timely and comprehensive disaster information. Motivated by this, we utilized multi-source heterogeneous data to assess the damage to traffic roads under extreme conditions and established a new framework for evaluating traffic roads in cities prone to flood disasters caused by rainstorms. The approach involves several steps: First, the surface area affected by precipitation is extracted using a threshold method constrained by confidence intervals derived from microwave remote sensing images. Second, disaster information is collected from the Sina Weibo platform, where social media information is screened and cleaned. A quantification table for road traffic loss assessment was defined, and a social media disaster information classification model combining text convolutional neural networks and attention mechanisms (TextCNN-Attention disaster information classification) was proposed. Finally, traffic road information on social media is matched with basic geographic data, the classification of traffic road disaster risk levels is visualized, and the assessment of traffic road disaster levels is completed based on multi-source heterogeneous data. Using the "7.20" rainstorm event in Henan Province as an example, this research categorizes the disaster's impact on traffic roads into five levels—particularly severe, severe, moderate, mild, and minimal—as derived from remote sensing image monitoring and social media information analysis. The evaluation framework for flood disaster traffic roads based on multi-source heterogeneous data provides important data support and methodological support for enhancing disaster management capabilities and systems.

Keywords: multi-source heterogeneity; flood disaster; social media information; TextCNN-Attention; traffic road; loss assessment

1. Introduction

The intensification of global climate change has led to the widespread, frequent, recurrent, and concurrent occurrence of extreme weather disasters in various regions [1–3]. In recent years, the losses and impacts of natural disasters caused by extreme weather

events have also intensified [4–6]. According to the "2023 Asian Climate Status" report released by the World Meteorological Organization, Asia experienced the highest incidence of disasters worldwide in 2023, primarily due to weather, climate, and hydrological factors. Floods and storms accounted for over 80% of these incidents, with floods and rainstorms causing the highest number of casualties and economic losses. Specifically, more than 60% of all disaster-related fatalities were caused by flooding. Urban areas, in particular, suffer significant disruptions from sudden, extreme rainstorms, leading to waterlogging and severely impacting road traffic. Rapid and precise identification of the spatial location, extent, and severity of the damage is crucial for enhancing the efficiency of post-disaster recovery efforts. Such measures are vitally important for establishing lifelines during disasters and reducing their overall impact [7,8]. As critical components of regional economic infrastructure, transportation roads play a pivotal role in the spread of disaster impacts. Consequently, the timely dissemination of traffic and road disaster assessment results is essential for effective emergency response and robust disaster risk management [9,10].

With the rapid advancement of remote sensing technology, remote sensing methods now enable the large-scale and rapid extraction of disaster-related information, characterized by low costs and dynamic detection capabilities [11,12]. Recent studies have focused on delineating flood inundation extents, primarily utilizing optical remote sensing images and synthetic-aperture radar (SAR) images for flood feature extraction [13–15]. Optical remote sensing offers direct imaging, better image quality, and abundant spectral data. Using spectral indices to identify areas affected by flooding and sediment deposition has yielded notable results [16–18]. However, optical remote sensing data are highly vulnerable to cloud cover and adverse weather conditions, which compromise the accurate extraction of disaster information. Frequently, existing cloud cover can also introduce significant errors in delineating inundation extents [19,20]. Microwave remote sensing, operable under all weather conditions, can penetrate clouds, snow, and fog, unaffected by meteorological factors. Flood information extraction methods using SAR imagery are typically categorized into traditional and deep-learning approaches [21,22]. Traditional methods are notably rapid, catering to the urgent needs following disasters but are less effective in complex terrains, often hampered by mountain shadows and sensor noise. Conversely, deep-learning methods have significantly enhanced extraction accuracy, offering improvements over issues associated with spectral interference from terrain and sensor anomalies. Nonetheless, the performance of deep-learning models is largely dependent on ample sample sizes, requiring further refinement and optimization, especially for models utilizing remote sensing data from diverse sources. The application of existing deep-learning models for rapid flood information extraction following brief, extreme weather-induced rainfall remains a subject for detailed investigation. Consequently, the development of a rapid flood information extraction system utilizing SAR image data represents a fundamental challenge addressed in this study.

In the era of digital intelligence, leveraging remote sensing for urban natural disaster emergency responses no longer suffices for comprehensive collection and rapid analysis of extreme natural disaster information. The advent of big data has revolutionized disaster management approaches and paradigms, introducing new research methodologies and strategies for urban flood prevention and governance. Social media crowdsourcing data, serving as an additional data source, offer a communication channel for reporting extreme natural disaster events. Its volume and spatial density often surpass that of traditional sensors [23,24]. Social media can rapidly aggregate information about sudden natural disasters in near real time, eliminating the need for deploying reconnaissance equipment or personnel. It provides timely disaster and geographic distribution information, enhancing the monitoring capabilities of Earth observation satellites. On one hand, it monitors social media users' attention and emotional responses to sudden natural disasters, providing valuable insights for emergency decision-making and public opinion management. On the other hand, the immediacy of social media data allows for a real-time understanding

of conditions in disaster-affected areas, supporting emergency assessments and aiding disaster response decision-making. Currently, experts and scholars have applied social media data to the fields of disaster prevention, mitigation, and emergency management. Among them, natural language processing technology is the key. The existing literature on natural disasters based on natural language processing technology mainly involves emotional analysis, sensitivity mapping, post-disaster recovery, loss assessment, and other aspects. Previous studies [25] have demonstrated the key role of social media in earthquake damage assessment and have defined a text-based damage assessment scale to indicate the potential utility of using social media data for rapid damage assessment. Researchers frequently employ text mining techniques to derive actionable insights during disasters. For instance, Yuan et al. (2018) created an index dictionary through semantic analysis to pinpoint damage-related tweets during Hurricane Matthew in Florida, illustrating the feasibility of using social media data to identify severely affected areas at the county level [26]. Another example utilized social media data for disaster loss evaluation, encompassing data preprocessing, fine-grained topic extraction, and quantitative damage estimation, and conducted correlation analysis at the urban level to link various themes with disaster losses [27]. Inspired by these findings, researchers have identified a strong correlation between social media activities and disaster damage [28,29]. Recent research efforts have significantly advanced the application of textual analysis to social media data in disaster assessment. However, these studies primarily focus on disaster risk assessment and seldom establish a correlation between textual analysis and estimates of traffic road damage. Moreover, traffic road damage assessment using social media information primarily involves text cleaning and processing of big data. Unlike news information classification, text classification methods in a disaster context face challenges due to the small amount of effective information, imbalanced sample data, and unclear differentiation scales between loss levels [8,30,31]. Thus, the principal aim of this study is to assess road damage using a restricted quantity of social media information.

Motivated by these insights, this paper aims to assess emergency flood traffic road damage by integrating analyses of social media data, remote sensing, and geographic information. By leveraging multi-source heterogeneous data, this approach aims to improve the accuracy of traffic road loss assessments in sudden natural disasters, enabling emergency personnel to devise more effective disaster relief strategies. In this study, a social media disaster information classification model combining text convolutional neural networks with attention mechanisms was developed (TextCNN-Attention disaster information classification). The main technical process is illustrated in Figure 1. This work contributes in two major ways:

(1) Flood impact scope identification of SAR images based on confidence intervals is proposed. The establishment of this threshold provides a scientific and reliable technique, enhancing the credibility of the model's predictions and results.
(2) A quantitative table for assessing road traffic loss based on social media disaster information was created, and a TextCNN-Attention disaster information classification model was developed. This model incorporates attention mechanisms and enhances prediction performance, accuracy, and stability by optimizing the size of convolutional kernels and the number of layers.

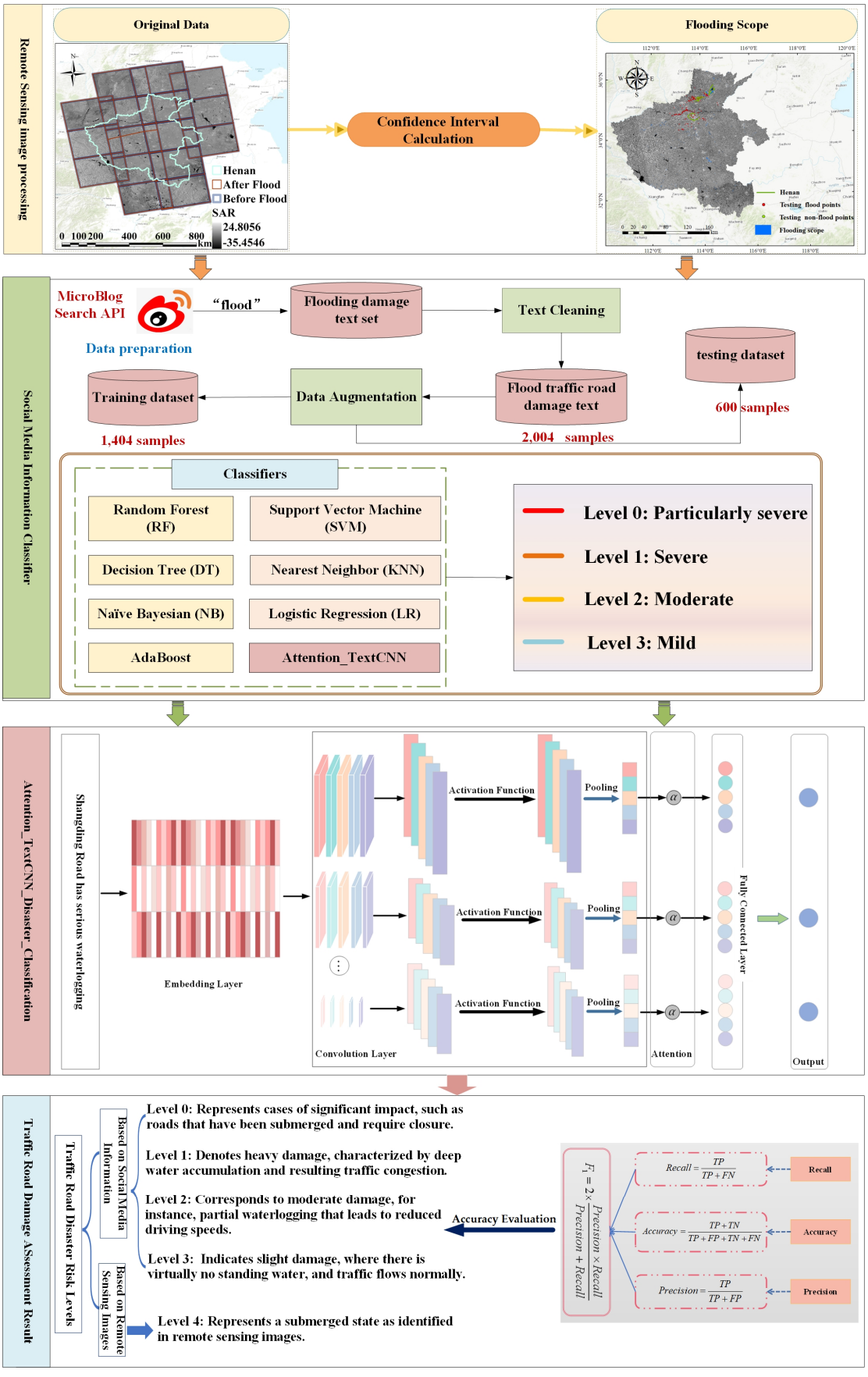


Figure 1. Leveraging multi−source data for emergency flood traffic road damage assessment flow.

2. Study Case and Data Collection

From 08:00 on 20 July 2021 to 06:00 on 21 July 2021, a severe rainstorm occurred in the north-central part of Henan Province, with extremely heavy rainfall recorded in areas of Zhengzhou, Xinxiang, Kaifeng, and others. Between 16:00 and 17:00 on July 20, the maximum hourly rainfall in the urban area of Zhengzhou reached 120–201.9 mm. The daily rainfall recorded at ten national meteorological observation stations in Zhengzhou, Xinxiang, and Kaifeng surpassed historical records. The intense rainfall affected approximately 13.9128 million people in Henan Province, resulting in 302 deaths and 50 individuals missing due to the disaster.

This study utilizes the Sina Weibo social platform to extract information on the rainstorm disaster in Henan. It allows users to access information through various mediums including the web, email, apps, instant messaging, SMS, PCs, and mobile devices, facilitating real-time sharing and transmission of information in text, images, videos, and other multimedia formats. Social media platforms, characterized by their rapid response, extensive coverage, and significant impact, are critical in managing large-scale sudden natural disasters. Scientific analysis of post-disaster social media data can effectively mitigate losses and social hazards, providing essential data for emergency management departments to understand the needs of affected areas. The data collection period spanned from 19 July 2021 to 24 July 2021, across Weibo and other platforms, yielding a total of 83,030 valid entries, including basic geographic information from Henan Province, as illustrated in Figure 2.

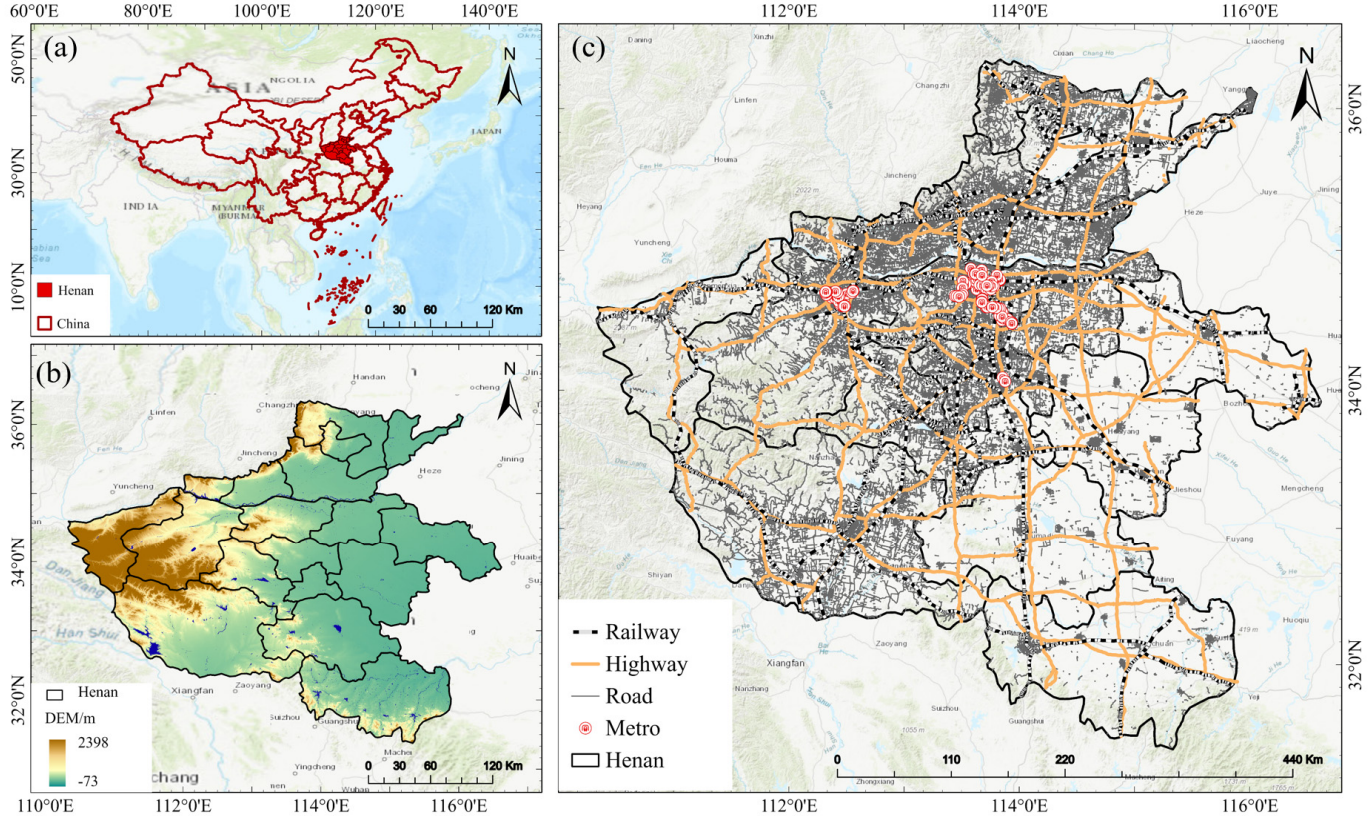


Figure 2. Study area information. (**a**) shows the geographic location of Henan Province, (**b**) is the digital elevation model, and (**c**) shows the road network of Henan Province.

3. Methodology

3.1. Flood Impact Scope Identification of SAR Images Based on Confidence Intervals

For remote sensing image data, Sentinel-1 synthetic-aperture radar (SAR) satellite imagery from the European Space Agency was employed to identify areas affected by waterlogging. VH polarized SAR images in IW mode GRD type HR were utilized, capturing data before the disaster from 1 July 2021 to 19 July 2021, and during the disaster from 20 July 2021 to 10 August 2021. Under the GEE platform, the extent of waterlogging was extracted using Sentinel-1 GRD image data, following preprocessing steps including orbit correction, ARD boundary noise removal, thermal noise removal, radiometric correction, terrain correction, and dB conversion. The study applied smoothing filters to SAR images to minimize speckle effects. A difference image was formed by dividing the post-disaster image by the pre-disaster image. Subsequently, the JRC dataset was imported, and areas with water for more than 10 months within a year were treated as permanent water bodies to eliminate background water. The flood threshold was determined within confidence interval constraints by selecting sample points.

A confidence interval is a commonly used method of interval estimation. For a dataset, where Ω is defined as the observation object, W is all possible observation results, and X is the actual observation value, X is essentially a random variable defined on Ω with values ranging over W. The confidence interval is defined by the functions $u(.)$ and $v(.)$, signifying that for an observation value $X = x$, its confidence interval is $(u(x), v(x))$. If the true value is w, then the confidence level is the probability c, expressed mathematically as follows:

$$c = Pr(\mathrm{u(X)} < \mathrm{w} < \mathrm{v(X)}) \tag{1}$$

where U = u(X) and V = v(X) are statistics, making the confidence interval a random interval: (U, V). For instance, constructing a value interval with 95% confidence implies that, in 100 parameter estimates, 95 are expected to fall within this interval. Confidence is typically denoted as 1- α. Thus, if $p < 0.05$, α represents statistical significance, and the confidence level is 0.95, equating to 95%. This is mathematically expressed as follows:

$$P(\mu \in [low, high]) = 1 - \alpha \tag{2}$$

Here, μ represents the estimated true value, and $P(\mu \in$ [low, high]) denotes the probability that the true value falls within the specified interval.

Assuming that the data follow a normal distribution, due to the symmetric nature of the distribution, the confidence interval can be expressed as $[\overline{X} - c, \overline{X} + c]$, where $\overline{X}$ is the sample mean, and c is the critical value to be calculated. This is applied in Formula (2) as follows:

$$P(\overline{X} - Z * \frac{\delta}{\sqrt{n}} \leq \mu \leq \overline{X} + Z * \frac{\delta}{\sqrt{n}}) = 1 - \alpha \tag{3}$$

In the formula, $\overline{X}$ is the sample mean, δ is the sample standard deviation, n is the sample size, α represents the confidence level, and P is the proportion value in the statistical sample.

3.2. Rapid Loss Assessment of Road Traffic in Flood Disasters Based on Social Media Data

3.2.1. Social Media Information Preprocessing

In the task of disaster loss analysis using social media data, data cleaning and purification are essential components of data preprocessing, significantly influencing both efficiency and outcomes. Initially, the original text often includes numerous non-essential characters (such as punctuation and spaces), which need to be removed, retaining only Chinese characters. After eliminating these characters, the text was segmented using Jieba's precise mode. In this mode, Jieba accurately divides the text into optimal word units, facilitating further analysis. To enhance text analysis quality, a stop word list was employed to filter the segmentation results. This list includes common conjunctions and particles that

add little analytical value, such as "we", "de", and "ma". The processed segments were then concatenated into a single string, separated by spaces, forming the preliminary disaster assessment text corpus. Furthermore, deduplication of the initial dataset is necessary. Assuming two texts, S1 and S2, are provided, Word2Vec is used to encode feature vectors. Using these encodings, the MinHash algorithm was used to perform a deduplication on social media text data. This method can measure the similarity between texts and efficiently purifies a large volume of collected social media data, thereby enhancing the accuracy of disaster data analysis. Based on this approach, social media information is matched with road information from OSM data to extract social media disaster information pertinent to roads. This process enables effective cleaning and purification of social media data, which aids in enhancing the accuracy of disaster analysis using social media data.

Disaster loss analysis via social media is essentially a multi-class text classification task, often challenged by small sample sizes and data imbalance between classes. To ensure balanced data across categories and maintain model classification accuracy, the study applied data augmentation. However, due to the specific nature of disaster information on social media, using random deletion methods may remove critical information, such as specific road names. Similarly, backtranslation for data augmentation might introduce semantic biases and compromise subsequent road information matching. To address these issues, this study designated road names as stop words to preserve essential road network information. The purpose of this operation is to avoid replacing road names with synonyms during data augmentation. On this basis, the synonym substitution method was used for data augmentation. The synonym library used is the Harbin Institute of Technology Synonym Word Forest. Additionally, random extraction enhancement was performed on each category of the original text. If the same text is selected multiple times, synonyms are used to prevent redundancy in the augmented data. Ultimately, the augmented text was integrated with the original corpus to create the final social media disaster information dataset.

3.2.2. Damage Scales and Text Labeling

To construct a rapid loss assessment model for road traffic in flood disasters using social media data, the initial step involves defining the classification of loss levels derived from social media data. This study utilizes emergency response plans for highway traffic emergencies to create a quantitative assessment table for road traffic losses, as illustrated in Table 1. The disaster levels of road networks are categorized into four grades: very serious, severe, relatively serious, and minor. Considering that some road disaster situations may not be reported by social media, remote sensing images identifying areas affected by waterlogging are used to enhance the assessment of the road network disaster status. The classifications are detailed as follows:

Level 0: Represents cases of significant impact, such as roads that have been submerged and require closure.

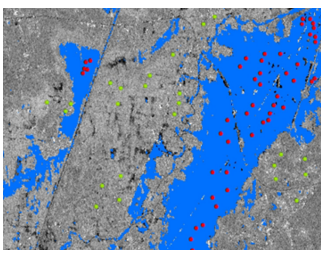
Level 1: Denotes heavy damage, characterized by deep water accumulation and resulting traffic congestion.

Level 2: Corresponds to moderate damage, for instance, partial waterlogging that leads to reduced driving speeds.

Level 3: Indicates slight damage, where there is virtually no standing water, and traffic flows normally.

Level 4: Represents a submerged state as identified in remote sensing images.

Table 1. Description and quantification of rapid assessment events for road traffic losses under flood disasters.

Damage Level	Event Description	Typical Descriptive Words	Case Description
Level 0—particularly severe	Due to sudden disaster events that may cause traffic damage, interruption, blockage, or a backlog of many vehicles; personnel retention, being trapped, or death; houses are submerged, collapsed, or tilted; and the estimated repair and disposal time is more than 24 h. When landslides, mudslides, or collapses occur, many people are stranded, and the resumption of operation and personnel evacuation are expected to take more than 48 h.	Serious/major/substantive/damage, serious injury, death of personnel, trapped, drowning, flooding, traffic paralysis, inability to pass, damage, collapse/collapse/collapse, landslide, mudslide flow, washout, urgent/urgent, severe disaster area, heavy injury, closure, flood discharge, embankment burst.	Severe flooding in Mihe Town, Gongyi, Henan Province. 
Level 1—severe	Due to unexpected events that may cause traffic damage, interruption, congestion, a large backlog of vehicles, inconvenient transportation, and personnel retention; the repair and disposal time is expected to be more than 12 h, resulting in a large amount of personnel retention. The resumption of operation and personnel evacuation are expected to take more than 24 h.	Some/extensive damage, multiple people injured, obstructed/damaged, congested, inconvenient transportation, deep mud/water accumulation, affected, requiring rescue.	Zhengzhou Zhongyuan Road West Fourth Ring Road is flooded with water. Traffic police have completed vehicle rescue and advised to avoid driving in the water. 
Level 2—moderate	When a sudden disaster occurs, the road traffic is smooth, slow, slightly muddy, slippery, and there is slight injury to personnel. Slow and slippery traffic.	Mild/minor/water accumulation, minor/minor/minor injury, walking slowly, slightly muddy, slippery, with small potholes, etc.	The one-kilometer section of Jindai Road in Zhengzhou is flooded with water, and the deepest point can submerge wheels halfway. 
Level 3—mild	In the event of a sudden disaster, there were no casualties, and there was no damage to the roads or houses. Rest areas and shelters were provided.	No/zero damage, no death, no damage, provide a venue/rest area/shelter/shelter, recover.	Zhengzhou Science and Technology Museum Parking Lot Refuge. 
Level 4—affected (interpreted from remote sensing images)	——	——	

3.2.3. Traffic Risk Classification Method Based on Social Media Information Data

In this study, the domain of traffic road classification using social media information encompasses four categories: Level 0, Level 1, Level 2, and Level 3. This study introduces a text classification model that integrates convolutional neural networks with attention mechanisms, termed the TextCNN-Attention disaster information classification model. This model is designed to optimize the utilization of both local features and global correlation information of text data, enhancing the efficiency and generalization capabilities of text classification tasks. Upon converting each word in social media information into a vector, the TextCNN-Attention disaster classification network classifies traffic damage information. This network comprises an embedding layer, a convolutional neural network module, an attention mechanism module, and a fully connected layer. The structure of the network is illustrated in Figure 3.

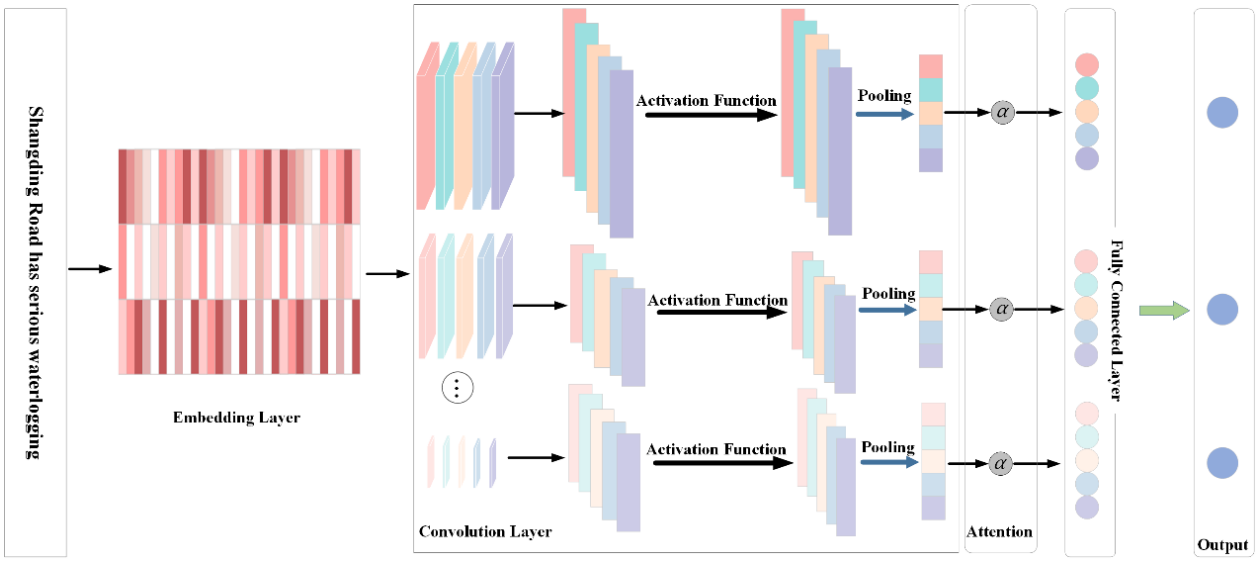


Figure 3. TextCNN-Attention disaster information classification flow.

Word embedding layer: Each word in the input text is transformed into a vector through spatial mapping, creating low-dimensional representations for each word. These vector representations are connected to form a two-dimensional matrix. Assuming the word vector representing the ith word in the sentence, the mathematical description is as follows:

$$x_{1:n} = x_1 \oplus x_2 \ldots \oplus x_n \tag{4}$$

where $\oplus$ represents the concatenation operator; usually, $x_{i:i+j}$ can be expressed as the concatenation of words x_i, x_{i+1}, x_{i+j}.

Convolutional module: This module extracts local features from the text. Each convolutional block includes a one-dimensional convolutional layer, a ReLU activation function, and a maximum pooling layer. The size and number of convolution kernels are adjusted to control the receptive field and the number of features extracted by the convolutional block. Convolutional layers are utilized to extract features between words, representing local sentence features. The ReLU activation function is employed to effectively capture and learn complex relationships and features in the input data, while the max pooling layer reduces feature dimensionality and highlights the most significant features. The mathematical description of a convolution operation includes a convolution kernel $w \in R^{h \times k}$, which uses a window size of $h \times k$ (where h is the number of words, and k is the encoding dimension) to generate a new feature. For example, feature c_i is generated by the words within the window from $x_{i:i+h\text{-}1}$, as shown in the following formula:

$$c_i = f(w \cdot x_{i:i+h-1} + b) \tag{5}$$

where $b \in R$ is the bias term, and f is a nonlinear function. This convolutional kernel traverses the words of the entire sentence $\{x_{1:h}, x_{2:h+1}, x_{n-h+1:n}\}$ to generate a feature map $c = [c_1, c_2, \ldots, c_{n-h+1}]$, where $c \in R_{n-h+1}$. The pooling layer employs maximum pooling, with the pooling size matching the dimensions of the feature map. The feature map is processed to extract the maximum value, resulting in the pooled feature map C. This map is then permuted, i.e., F = Permute (C).

Attention mechanism module: Following the convolution module, an attention mechanism is introduced, enhancing the model's performance and interpretability by dynamically focusing on critical text segments. The attention module includes a learnable parameter matrix to compute the attention weights for each feature. The weighted feature representation, which incorporates global correlation information, is derived by calculating the weighted average of the feature and attention weights. Its mathematical description is as follows:

$$\begin{aligned} e_t &= \tanh(W \cdot F + b) \\ \alpha_t &= \frac{\exp(e_t)}{\sum_{t'} \exp(e_{t'})} \\ V &= \sum_t \alpha_t \cdot F_t \end{aligned} \tag{6}$$

In the formula, e_t is the attention score, W is the weight matrix, α_t is the attention weight, and V represents the weighted feature.

Finally, these weighted feature representations are fed into a linear classifier to determine the text's category probabilities. The model's accuracy is enhanced using a cross-entropy loss function to gauge the discrepancy between the model output and actual labels, and model parameters are refined via the backpropagation algorithm to minimize loss. The entire training regimen is conducted using an optimizer, specifically the AdamW optimizer, which updates model parameters and boosts the model's convergence speed and performance by fine-tuning the learning rate and other hyperparameters.

3.3. Accuracy Evaluation

Here, accuracy, precision, recall, and F1 score [25,32] are metrics used to evaluate the accuracy of remote sensing image inundation range recognition classification and the performance of traffic risk level classification based on social media information. Here, TP represents the number of true positives, TN is the number of true negatives, FP is the number of false positives, and FN is the number of false negatives.

Precision is defined as the ratio of true positives to the total number of items classified as positive, expressed in Formula (7):

$$Precision = \frac{\mathrm{TP}}{\mathrm{TP} + \mathrm{FP}} \tag{7}$$

Recall (sensitivity) is the ratio of true positives to all actual positive cases, as defined in Formula (8):

$$Recall = \frac{\mathrm{TP}}{\mathrm{TP} + \mathrm{FN}} \tag{8}$$

The F1 score, the harmonic mean of precision and recall, evaluates the overall efficacy of classification models. It ranges from 0 to 1, with higher values indicating better model performance, as shown in Formula (9):

$$F1\ score = \frac{2}{\mathrm{Precision}^{-1} + \mathrm{Recall}^{-1}} = 2 \times \frac{\mathrm{Precision} \times \mathrm{Recall}}{\mathrm{Precision} + \mathrm{Recall}} \tag{9}$$

Furthermore, the accuracy for each model was computed across different levels of damage. Accuracy is the proportion of correctly classified samples to the total number of samples, serving as a comprehensive statistical measure, mathematically expressed in Formula (10):

$$Accuracy = \frac{\mathrm{TP} + \mathrm{TN}}{\text{total sample}} \tag{10}$$

4. Experimental Results and Analysis

4.1. Short-Term Rainstorm Flood Disaster Information Extraction and Analysis

This study extracted the surface area affected by short-term rainstorms based on confidence intervals to address the rapid emergency response needs for urban waterlogging resulting from such events. To further verify the recognition accuracy of SAR images affected by rainstorms based on confidence intervals, 525 flood points and 300 non-flood points were identified by selecting sample point data through visual interpretation, as depicted in Figure 4. The flood point sample data were distributed in a ratio of approximately 6:4, with 60% of the flood point data used in threshold determination based on confidence intervals. The average value of the sample point data was 1.18, the standard deviation was 0.08, and the final threshold was set at 1.19. This threshold was utilized to identify areas affected by short-term rainstorm-induced urban waterlogging, as illustrated in Figure 4. The main area impacted by the flooding is in the northeast of Henan Province (specifically Xinxiang City and Hebi City), where the flood impact was concentrated in densely populated urban communities, resulting in significant economic and property losses and posing threats to human safety. The experiment evaluated the performance of the proposed flood impact range recognition using precision, recall, F1 score, and accuracy metrics. The calculated results for precision, recall, F1 score, and accuracy were 0.89, 0.86, 0.88, and 0.87, respectively. These evaluation results indicate that the extraction accuracy of the flood impact range is satisfactory, suitable for rapid emergency response following short-term rainstorm disasters, and provides data support and methodological backing for enhancing post-disaster governance capabilities.

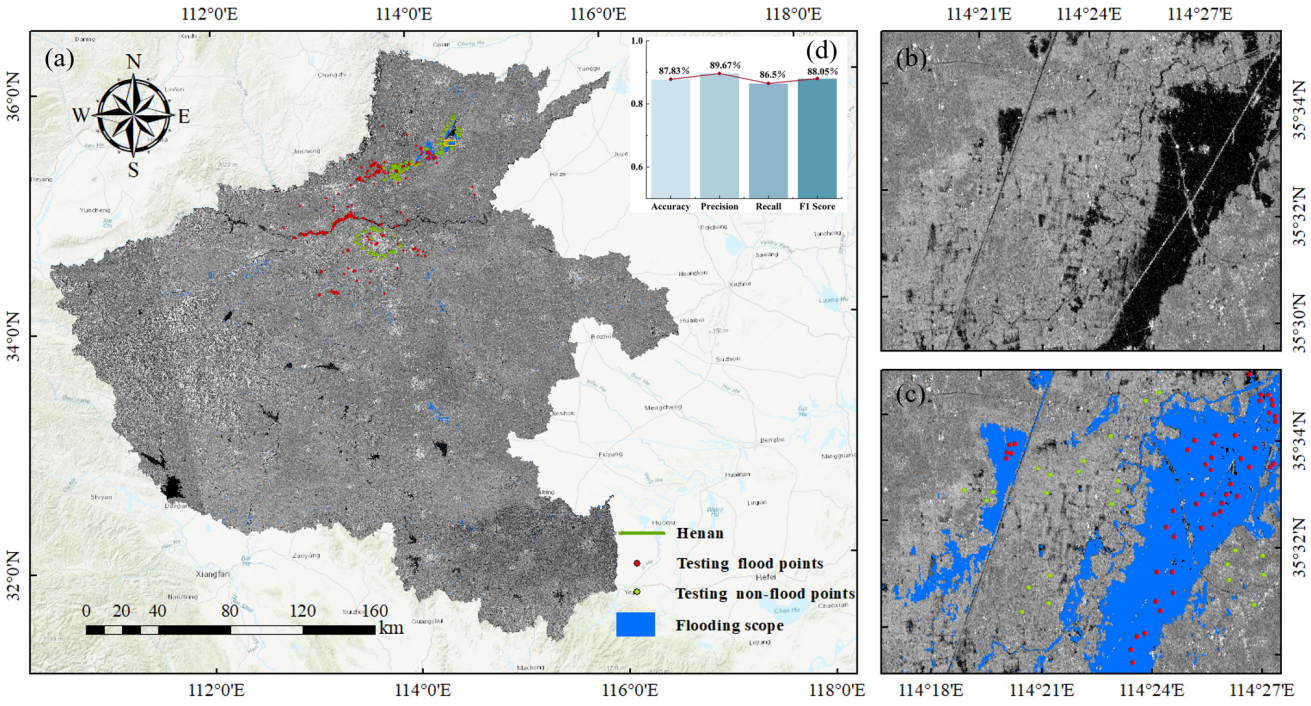


Figure 4. Flood impact scope identification result and accuracy evaluation. (**a**) is the flood impact scope identification result and distribution of sample points. (**b**) is a partial enlargement of the post-disaster SAR data of Figure 4a. (**c**) is a partial enlargement of the flood impact scope identification result. (**d**) is the accuracy evaluation of flood impact scope identification.

4.2. Processing and Analysis of Social Media Data

The study collected 83,030 pieces of social media information regarding the 20 July 2021 flood and rainstorm disaster in Henan Province. After preprocessing, purification, and cleaning, 826 pieces of social media information related to road network damage were identified. To address the potential underfitting due to small sample sizes in multi-

classification tasks, the sample data were augmented, increasing the original count of 826 to 2004, thus achieving 1178 data augmentations. Specifically, the augmentation included 447 pieces for Level 1, representing 38% of the total augmentations; 345 for Level 2, accounting for 29%; and 386 for Level 3, making up 33%. Based on the damage level, manual classification was conducted, and the sample data are detailed in Table 2.

Table 2. Example of social media data preprocessing results and labeling situation.

Social Media Information Original Text	Preprocessed Results	Label
#The rainstorm in Zhengzhou this summer # Audience feedback: there is serious water accumulation near Shangding Road, East Fourth Ring Road, Zhengzhou, almost no roof# Rainstorm Screens in Henan # # Microblog Video of rainstorm in Henan Province # LMyRadio.	There is severe waterlogging near Shangding Road in the East Fourth Ring Road of Zhengzhou, with almost no water passing through the roof.	0
#The rainstorm in Zhengzhou this summer # Audience feedback: the north ring bridge of Huayuan Road in Zhengzhou is impassable# Rainstorm Screens in Henan # # Microblog Video of rainstorm in Henan Province # LMyRadio.	Unable to pass under the North Ring Bridge of Huayuan Road in Zhengzhou.	0
#Rainstorm in Zhengzhou this summer # Audience feedback, the depth of non-motorized vehicle lane of Zhengzhou Agricultural Road via No. 5 Road is deep# Rainstorm Screens in Henan # # Henan Province Faces rainstorm # LMyRadio Weibo Video	Zhengzhou Agricultural Road passes through the water depth of the fifth non-motorized lane.	1
#Henan rainstorm # # Zhengzhou rainstorm # There is deep ponding at the future intersection of Zhengzhou Jinshui Road, please pay attention to passing vehicles! Xiaohui's Weibo video on the road	There will be deep water accumulation at the future intersection of Jinshui Road. Vehicles should pay attention.	1
[# Zhengzhou # One section of the road has accumulated water above the knee of a man] # rainstorm in Henan # On July 19, a reporter found that the Jindai Road in Zhengzhou was one kilometer away from the South Fourth Ring Road. There was a serious accumulation of water on the driveway of Jindai Road. There was nearly one kilometer of water on the north-south two-way six lanes, and the deepest part could submerge half of the wheels. The outer lane of the two-way road had deeper water. If the motor vehicle ran a little faster, it would stir up water spray twice higher than the body. At present, the water accumulation situation is still ongoing, and the on-site reporter did not see the pumping operation. Why is the water accumulation in this section so severe? Why is there no drainage operation? Journalists from Henan Traffic Radio will also continue to pay attention. Weibo Video of Henan Traffic Radio	The one-kilometer section of Jindai Road in Zhengzhou is flooded with water, and the deepest point can submerge half of the wheels.	2
#Pay attention to the heavy rainstorm in Henan # [Zhengzhou South Third Ring Road and other water accumulation points have been opened up] At 6:40 this morning, the water accumulation points in the South Third Ring Road jointly pumped and drained by Wuhan Water Group, the East Lake High tech Zone and the Huangpi District Water Affairs Department completed the task of pumping and draining, and handed it over to the local government for cleaning up as required by the local government. Following the opening of the waterlogging points on the South Third Ring Road, the Wuhan drainage rescue team has completed a total of 7 important waterlogging point drainage tasks, ensuring the restoration of urban main road traffic.	Zhengzhou South Third Ring Road and other waterlogging points have been gradually connected.	3

In the analysis of traffic road risk assessment based on social media data, the target domain comprises four categories: Level 0, Level 1, Level 2, and Level 3. After encoding feature vectors using Word2Vec, the TextCNN-Attention model was employed to classify social media information pertaining to flood disasters, and its performance was compared with various machine-learning classifiers. The comparative classifiers used in this study include Nearest Neighbor (KNN), Logistic Regression (LR), Naïve Bayesian (NB), Decision Tree (DT), Support Vector Machine (SVM), Random Forest (RF), Adaboost algorithm, and TextCNN. The classification results are summarized in Table 3.

Table 3. Classification performance.

Dataset	Method	Precision	Recall	F1 Score	Accuracy
Original dataset	KNN	0.76	0.75	0.70	0.75
	LR	0.66	0.68	0.59	0.68
	NB	0/57	0.66	0.55	0.66
	DT	0.79	0.71	0.73	0.71
	SVM	0.76	0.76	0.74	0.76
	RF	0.71	0.73	0.69	0.73
	AdaBoost	0.75	0.69	0.70	0.69
	TextCNN	0.80	0.54	0.56	0.73
	TextCNN-Attention	0.95	0.95	0.95	0.94
Augmented dataset	KNN	0.79	0.79	0.79	0.79
	LR	0.88	0.88	0.88	0.88
	NB	0.84	0.84	0.83	0.84
	DT	0.86	0.86	0.86	0.86
	SVM	0.91	0.91	0.91	0.91
	RF	0.89	0.88	0.88	0.88
	AdaBoost	0.75	0.62	0.62	0.62
	TextCNN	0.82	0.60	0.61	0.76
	TextCNN-Attention	0.97	0.97	0.97	0.96

The experimental results indicate that the classification performance of KNN on the original dataset is moderate, with similar metrics but a low F1 score, suggesting that the model may underperform in certain categories. Logistic Regression (LR) also exhibits average performance on the original dataset, with a relatively low F1 score and precision, indicating difficulties in managing category imbalance. Naive Bayes shows notably low precision, potentially due to poor prediction accuracy or overfitting to specific categories. The Decision Tree model performs well on the original dataset, particularly in terms of higher precision and F1 score. The Support Vector Machine (SVM) displays balanced performance across all metrics on the original dataset, demonstrating robust classification capabilities. Random Forest (RF) has slightly lower classification accuracy compared to SVM and the Decision Tree model across various metrics. AdaBoost's performance on the augmented dataset has deteriorated, especially in terms of recall and F1 score, likely due to overfitting or issues stemming from data augmentation. The lower F1 score of the TextCNN model may result from imbalanced data and suboptimal parameter settings. The TextCNN-Attention model exhibits the strongest performance on both the original and augmented datasets, with metrics surpassing 96% following data augmentation. Overall, data augmentation has improved the performance of most models, underscoring its significance in enhancing model generalization and effectiveness, particularly for traditional machine-learning models. Future efforts should concentrate on refining data augmentation techniques for models such as AdaBoost and investigating the interplay between different data augmentation methods and various machine-learning algorithms.

The TextCNN-Attention disaster information classification network analyzes the damage to traffic roads following a short-term rainstorm, with a specific focus on 720 traffic road networks in Henan Province affected by the event. The road network in Henan Province encompasses four categories: railway, expressway, highway, and subway. The total length of traffic roads impacted by the rainstorm is approximately 10,272.47 km. Of this, railways affected based on social media information cover about 181.47 km, accounting for 1.39% of the total railway length. Similarly, microwave remote sensing data indicate that railways were affected over a length of 181.38 km, also representing 1.39% of the total. For expressways, social media data show that about 149.01 km was impacted, constituting 0.66% of their total length, with 62.02 km classified as severely affected. Remote sensing data suggest a total affected expressway length of 86.99 km, accounting for 0.39% of the total expressway

length. The length of affected highways, as reported on social media, is approximately 9688.04 km, constituting 3.99% of the total, with severely affected sections amounting to 2570.97 km or 1.06% of the total highway length. Remote sensing data indicate that affected highways extend to 1888.77 km, or 0.78% of the total. The subway system was significantly impacted, with social media information revealing that approximately 253.95 km, or 42.10% of the total subway length, was affected by the rainstorm. Severely affected subway sections spanned 102.41 km, representing 16.98% of the total length. Differences between the statistical results from social media information and remote sensing imagery analysis exist primarily because social media data can record roads impacted by disasters in real time more effectively. They may include more localized details, such as minor roads or temporary closures. Often, social media disaster information merely lists the names of affected roads, leading to the calculation of their entire lengths during the statistical process, thus introducing deviations in the length statistics. While microwave remote sensing imagery covers a broader geographic area, its time resolution may not suffice for real-time disaster statistics. Consequently, differences may arise in the identification of specific roads and the assessment of affected conditions. Remote sensing imagery might not capture all actual traffic disruptions, especially those occurring over short periods. The visualization of these results is displayed in Figure 5.

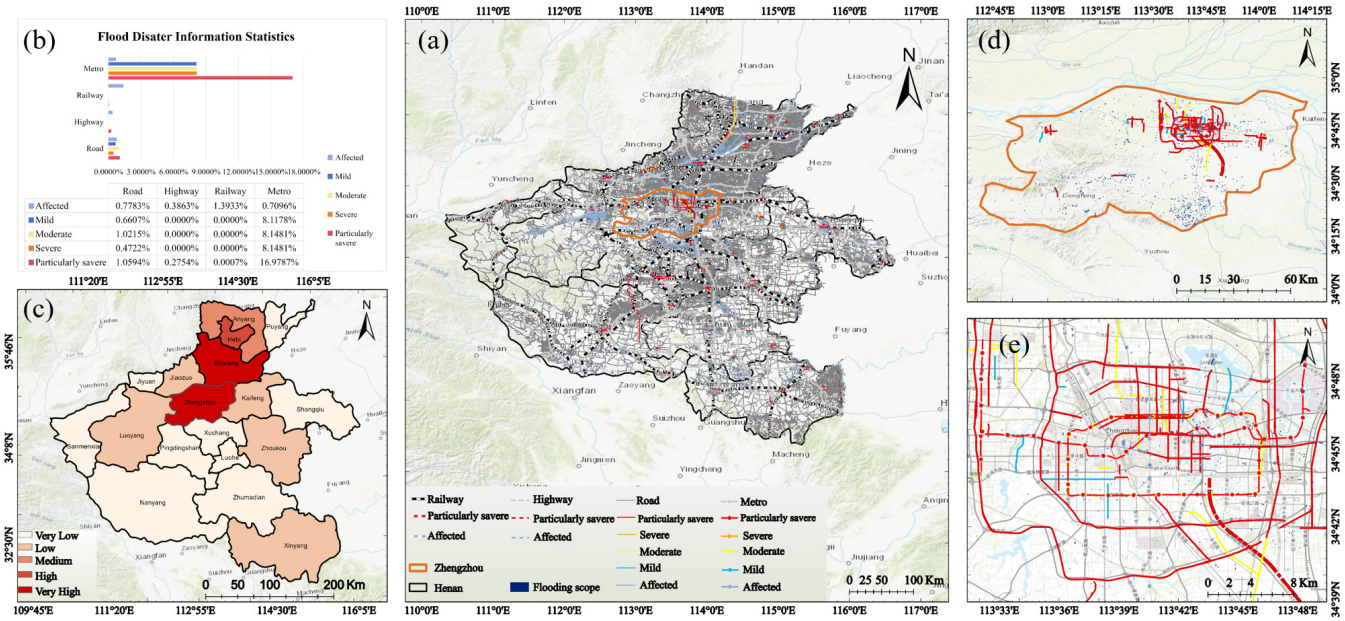


Figure 5. Visualization results of the disaster situation in the road network of Henan Province. (**a**) is the traffic road damage assessment of Henan Province, (**b**) is the traffic road damage assessment statistical results of Henan Province, (**c**) is social media information posting popularity statistics, (**d**) is the traffic road damage assessment of Zhengzhou City, and (**e**) is the localized amplification result of traffic road damage assessment of Zhengzhou City.

5. Discussion

5.1. Theoretical Contributions and Implications for Practice

The integration of multi-source data and multidisciplinary theoretical approaches has been extensively explored in the study of urban flooding caused by heavy rainstorms. For instance, multi-source remote sensing imagery and machine-learning models have been utilized to detect and analyze storm-induced urban flooding [33,34]. Despite this, challenges in data integration and computational speed persist. In response, this study employs a confidence-interval-constrained thresholding method, which is simple to operate, offers faster processing speeds, and is more suitable for large-scale datasets. Compared to the water identification algorithm [35], our approach further refines the precision of

threshold determination by incorporating confidence interval constraints, thus addressing a significant limitation of over-reliance on sample data.

For the rapid assessment of road damage due to flooding, existing studies have explored the integration of Geographic Information Systems (GISs) and social media data. For instance, social media data have been used to assess the impact of disasters on infrastructure; however, this method encounters challenges in data cleaning and classification model precision [36]. Our study improves the accuracy of multi-class classification in small-sample problems through the TextCNN-Attention disaster information classification model and is the first to merge social media data with SAR imagery for a joint assessment of road damage. Compared to traditional methods, this approach provides a more time-sensitive response, enabling rapid action following short-term heavy rainstorms.

Additionally, our study enhances the real-time aggregation of disaster information from social media to complement remote sensing imagery, notably improving accuracy in temporal and spatial dimensions. Unlike methods that rely on a single data source [37,38], the multi-source data fusion in our study augments the completeness of disaster information and the accuracy of damage assessments.

5.2. Limitations and Future Research

This experiment has shifted the approach of disaster data collection and mining, enabling a vast amount of "blind data" to assert its "data sovereignty." This transition aids in gaining crucial buffer time for disaster risk response, transforming from remote sensing big data to multi-source heterogeneous disaster data, and applying disaster big data to facilitate timely and rapid loss assessments following short-term rainstorms. In this experiment, the SAR radiation values of the sample data were relatively concentrated, with minimal variation in threshold determination based on the confidence interval. Additionally, a semi-automatic interpretation method was employed to address the inherent band problem in SAR data. Future research will consider using adaptive thresholds to enhance the accuracy of water body recognition. Compared to Earth observation data, the robustness and accuracy of integrating Internet social media data in sudden natural disaster risk assessments remain central to further in-depth studies. The social media data primarily originate from the Weibo platform. Future experiments will incorporate data from additional social media platforms to enhance the representativeness of the data and the robustness of the model. This study uniformly processed stop words for social media data. However, due to the wide variety of social media data sources and formats, applying this processing method uniformly to subsequent disaster events may not be feasible. Monitoring updates to the stop word database for disaster public opinion information will be a foundational task moving forward. This study primarily visualized the damage in affected areas based on location feedback from text content, which differs from the user's posting location, home location, or registration location, ensuring the reliability of spatial distribution in disaster damage information. The overall evaluation depends on the dataset's quantity and quality; insufficient data or inadequate data cleaning may introduce biases into the final assessment. Ongoing efforts will focus on improving text classification models to better handle the challenges of small-sample data and high-precision classification in social media information. Future research will also emphasize the development of multimodal large language models, which excel in text generation, semantic understanding, and are effective in cross-modal information fusion and human–computer interaction. A key future challenge will be selecting appropriate models based on actual needs in specific disaster assessment scenarios.

6. Conclusions

Flood disasters caused by short-term severe precipitation have inflicted significant losses on social and economic development. This study, focusing on the extreme rainstorm in Henan Province from 17 to 23 July 2021, applied multi-source heterogeneous data to thoroughly assess the risk to traffic roads from short-term urban flood disasters. This

approach can provide valuable insights for utilizing multi-source heterogeneous data to analyze damage to urban waterlogged traffic roads from short-term rainstorms and offers a new perspective on the potential of using social media to assess expressway damage.

(1) This study used a confidence-interval-based threshold algorithm to identify the scope of flood impact, enabling rapid responses to sudden disasters. The evaluation metrics, including precision, recall, F1 score, and accuracy, were recorded to be 0.89, 0.86, 0.88, and 0.87, respectively. This method allows for swift and targeted analysis of the impact range of short-term flood disasters, providing essential data support for disaster emergency response and post-disaster rescue efforts.

(2) This study can improve the accuracy of addressing small-sample multi-classification problems by filtering and cleaning social media data and integrating a text classification model based on convolutional neural networks and attention mechanisms (TextCNN-Attention) following sample enhancement. Combined with the comprehensive analysis of microwave remote sensing images, traffic road risk grades for short-term rainstorm flood disasters are categorized into five levels. Consequently, the accuracy of the TextCNN-Attention model in classifying these risk grades reaches 96%. Additionally, a quantitative table for road traffic loss assessment based on social media information has been completed. The assessment method proposed by the TextCNN-Attention model demonstrates high transferability for traffic road risk assessment in various disaster contexts, offering a robust tool for estimating traffic road risk in other regions affected by short-term rainstorm floods.

Author Contributions: Hong Zhu proposed the methodology and wrote the manuscript. Jian Meng and Jiaqi Yao contributed to improving the methodology and were the corresponding authors. Nan Xu helped edit and improve the manuscript. All authors have read and agreed to the published version of the manuscript.

Funding: This research was jointly supported by grants from the Science and Technology Research and Development Plan Self-Fund Program of Langfang (Grant No. 2024011025); Hebei Key Laboratory of Resource and Environmental Disaster Mechanism and Risk Monitoring (Grant No.FZ248204); the Hebei Natural Science Foundation (Grant No.D2020512001); by the National Natural Science Foundation of China (Grant No.42101343); by the National Natural Science Foundation of China (Grant No. 5047803); the National natural disaster risk remote sensing monitoring prewarning and emergency application platform construction (Grant No. 2021YFB3901204); the Science technology research and development plan self-fund program of Langfang (Grant No. 2022011020); the Hebei Province Science and Technology Research Project (Grant No. Z2020119); and the Fundamental Research Funds for the Central Universities (Grant No. ZY20200202).

Data Availability Statement: The data are not publicly available due to privacy restrictions.

Conflicts of Interest: Author Jian Meng is employed by the Beijing Disaster Prevention Science and Technology, Co., Ltd. The remaining authors declare that the research was conducted in the absence of any commercial or financial relationships that could be construed as a potential conflict of interest.

References

1. Wang, T.; Wang, H.; Wang, Z.; Huang, J. Dynamic risk assessment of urban flood disasters based on functional area division—A case study in Shenzhen, China. *J. Environ. Manag.* **2023**, *345*, 118787. [CrossRef] [PubMed]
2. Xu, N.; Lu, H.; Li, W.; Gong, P. Natural lakes dominate global water storage variability. *Sci. Bull.* **2024**, *69*, 1016–1019. [CrossRef] [PubMed]
3. Zhu, H.; Yao, J.; Meng, J.; Cui, C.; Wang, M.; Yang, R. A Method to Construct an Environmental Vulnerability Model Based on Multi-Source Data to Evaluate the Hazard of Short-Term Precipitation-Induced Flooding. *Remote Sens.* **2023**, *15*, 1609. [CrossRef]
4. Rodell, M.; Li, B. Changing intensity of hydroclimatic extreme events revealed by GRACE and GRACE-FO. *Nat. Water* **2023**, *1*, 241–248. [CrossRef]
5. Lan, H.; Zhao, Z.; Li, L.; Li, J.; Fu, B.; Tian, N.; Lai, R.; Zhou, S.; Zhu, Y.; Zhang, F.; et al. Climate change drives flooding risk increases in the Yellow River Basin. *Geogr. Sustain.* **2024**, *5*, 193–199. [CrossRef]
6. Dottori, F.; Szewczyk, W.; Ciscar, J.-C.; Zhao, F.; Alfieri, L.; Hirabayashi, Y.; Bianchi, A.; Mongelli, I.; Frieler, K.; Betts, R.A.; et al. Increased human and economic losses from river flooding with anthropogenic warming. *Nat. Clim. Chang.* **2018**, *8*, 781–786. [CrossRef]

7. Roy, K.C.; Hasan, S.; Culotta, A.; Eluru, N. Predicting traffic demand during hurricane evacuation using Real-time data from transportation systems and social media. *Transp. Res. Part C Emerg. Technol.* **2021**, *131*, 103339. [CrossRef]
8. Chen, Y.; Ji, W. Enhancing situational assessment of critical infrastructure following disasters using social media. *J. Manag. Eng.* **2021**, *37*, 04021058. [CrossRef]
9. He, H.; Li, R.; Pei, J.; Bilodeau, J.P.; Huang, G. Current overview of impact analysis and risk assessment of urban pluvial flood on road traffic. *Sustain. Cities Soc.* **2023**, *99*, 104993. [CrossRef]
10. Cartes, P.; Navarro, T.E.; Giné, A.C.; Binet, E.A. A cost-benefit approach to recover the performance of roads affected by natural disasters. *Int. J. Disaster Risk Reduct.* **2021**, *53*, 102014. [CrossRef]
11. Zhang, X.; Song, Y.; Nam, W.H.; Huang, T.; Gu, X.; Zeng, J.; Huang, S.; Chen, N.; Yan, Z.; Niyogi, D. Data fusion of satellite imagery and downscaling for generating highly fine-scale precipitation. *J. Hydrol.* **2024**, *631*, 130665. [CrossRef]
12. Kazemi Garajeh, M.; Haji, F.; Tohidfar, M.; Sadeqi, A.; Ahmadi, R.; Kariminejad, N. Spatiotemporal monitoring of climate change impacts on water resources using an integrated approach of remote sensing and Google Earth Engine. *Sci. Rep.* **2024**, *14*, 5469. [CrossRef] [PubMed]
13. Shen, X.; Wang, D.; Mao, K.; Anagnostou, E.; Hong, Y. Inundation extent mapping by synthetic aperture radar: A review. *Remote Sens.* **2019**, *11*, 879. [CrossRef]
14. Jiang, X.; Liang, S.; He, X.; Ziegler, A.D.; Lin, P.; Pan, M.; Wang, D.; Zou, J.; Hao, D.; Mao, G.; et al. Rapid and large-scale mapping of flood inundation via integrating spaceborne synthetic aperture radar imagery with unsupervised deep learning. *ISPRS J. Photogramm. Remote Sens.* **2021**, *178*, 36–50. [CrossRef]
15. Serpico, S.B.; Dellepiane, S.; Boni, G.; Moser, G.; Angiati, E.; Rudari, R. Information extraction from remote sensing images for flood monitoring and damage evaluation. *Proc. IEEE* **2012**, *100*, 2946–2970. [CrossRef]
16. Li, Y.; Dang, B.; Zhang, Y.; Du, Z. Water body classification from high-resolution optical remote sensing imagery: Achievements and perspectives. *ISPRS J. Photogramm. Remote Sens.* **2022**, *187*, 306–327. [CrossRef]
17. Kang, J.; Guan, H.; Ma, L.; Wang, L.; Xu, Z.; Li, J. WaterFormer: A coupled transformer and CNN network for waterbody detection in optical remotely-sensed imagery. *ISPRS J. Photogramm. Remote Sens.* **2023**, *206*, 222–241. [CrossRef]
18. Yao, J.; Sun, S.; Zhai, H.; Feger, K.-H.; Zhang, L.; Tang, X.; Li, G.; Wang, Q. Dynamic monitoring of the largest reservoir in North China based on multi-source satellite remote sensing from 2013 to 2022: Water area, water level, water storage and water quality. *Ecol. Indic.* **2022**, *144*, 109470. [CrossRef]
19. Mohseni, F.; Saba, F.; Mirmazloumi, S.M.; Amani, M.; Mokhtarzade, M.; Jamali, S.; Mahdavi, S. Ocean water quality monitoring using remote sensing techniques: A review. *Mar. Environ. Res.* **2022**, *180*, 105701. [CrossRef]
20. Mayer, T.; Poortinga, A.; Bhandari, B.; Nicolau, A.P.; Markert, K.; Thwal, N.S.; Markert, A.; Haag, A.; Kilbride, J.; Chishtie, F.; et al. Deep learning approach for Sentinel-1 surface water mapping leveraging Google Earth Engine. *ISPRS Open J. Photogramm. Remote Sens.* **2021**, *2*, 100005. [CrossRef]
21. Mcfeeters, S.K. The use of the Normalized Difference Water Index (NDWI) in the delineation of open water features. *Int. J. Remote Sens.* **1996**, *17*, 1425–1432. [CrossRef]
22. Li, H.; Xu, Z.; Zhou, Y.; He, X.; He, M. Flood Monitoring Using Sentinel-1 SAR for Agricultural Disaster Assessment in Poyang Lake Region. *Remote Sens.* **2023**, *15*, 5247. [CrossRef]
23. Ghouri, A.Y.; Khan, A.; Raoof, H.; Miandad, M.; Rehman, G. Flood Mapping Using the Sentinel-1 SAR Dataset and Application of the Change Detection Approach Technique (CDAT) to the Google Earth Engine in Sindh Province, Pakistan. *Ecol. Quest.* **2024**, *35*, 1–18.
24. Yang, T.; Xie, J.; Li, G.; Zhang, L.; Mou, N.; Wang, H.; Zhang, X.; Wang, X. Extracting Disaster-Related Location Information through Social Media to Assist Remote Sensing for Disaster Analysis: The Case of the Flood Disaster in the Yangtze River Basin in China in 2020. *Remote Sens.* **2022**, *14*, 1199. [CrossRef]
25. Li, L.; Bensi, M.; Cui, Q.; Baecher, G.B.; Huang, Y. Social media crowdsourcing for rapid damage assessment following a sudden-onset natural hazard event. *Int. J. Inf. Manag.* **2021**, *60*, 102378. [CrossRef]
26. Yuan, F.; Liu, R. Feasibility study of using crowdsourcing to identify critical affected areas for rapid damage assessment: Hurricane Matthew case study. *Int. J. Disaster Risk Reduct.* **2018**, *28*, 758–767. [CrossRef]
27. Dou, M.; Wang, Y.; Gu, Y.; Dong, S.; Qiao, M.; Deng, Y. Disaster damage assessment based on fine-grained topics in social media. *Comput. Geosci.* **2021**, *156*, 104893. [CrossRef]
28. Hao, H.; Wang, Y. Leveraging multimodal social media data for rapid disaster damage assessment. *Int. J. Disaster Risk Reduct.* **2020**, *51*, 101760. [CrossRef]
29. Ogie, R.I.; James, S.; Moore, A.; Dilworth, T.; Amirghasemi, M.; Whittaker, J. Social media use in disaster recovery: A systematic literature review. *Int. J. Dis. Risk Reduct.* **2022**, *70*, 102783. [CrossRef]
30. Lozano, J.M.; Tien, I. Data collection tools for post-disaster damage assessment of building and lifeline infrastructure systems. *Int. J. Disaster Risk Reduct.* **2023**, *94*, 103819. [CrossRef]
31. Li, L.; Bensi, M.; Baecher, G. Exploring the potential of social media crowdsourcing for post-earthquake damage assessment. *Int. J. Disaster Risk Reduct.* **2023**, *98*, 104062. [CrossRef]
32. Lever, J.; Krzywinski, M.; Altman, N. Classification evaluation. *Nat. Methods* **2016**, *13*, 603–604. [CrossRef]
33. McCormack, T.; Campanyà, J.; Naughton, O. A methodology for mapping annual flood extent using multi-temporal Sentinel-1 imagery. *Remote Sens. Environ.* **2022**, *282*, 113273. [CrossRef]

34. Tan, W.; Qin, N.; Zhang, Y.; McGrath, H.; Fortin, M.; Li, J. A rapid high-resolution multi-sensory urban flood mapping framework via DEM upscaling. *Remote Sens. Environ.* **2024**, *301*, 113956. [CrossRef]
35. Rahaman, S.N.; Shermin, N. Identifying the effect of monsoon floods on vegetation and land surface temperature by using Google Earth Engine. *Urban Clim.* **2022**, *43*, 101162. [CrossRef]
36. Loli, M.; Kefalas, G.; Dafis, S.; Mitoulis, S.A.; Schmidt, F. Bridge-specific flood risk assessment of transport networks using GIS and remotely sensed data. *Sci. Total Environ.* **2022**, *850*, 157976. [CrossRef]
37. Fang, J.; Hu, J.; Shi, X.; Zhao, L. Assessing disaster impacts and response using social media data in China: A case study of 2016 Wuhan rainstorm. *Int. J. Disaster Risk Reduct.* **2019**, *34*, 275–282. [CrossRef]
38. Tan, L.; Schultz, D.M. Damage classification and recovery analysis of the Chongqing, China, floods of August 2020 based on social-media data. *J. Clean. Prod.* **2021**, *313*, 127882. [CrossRef]

Disclaimer/Publisher's Note: The statements, opinions and data contained in all publications are solely those of the individual author(s) and contributor(s) and not of MDPI and/or the editor(s). MDPI and/or the editor(s) disclaim responsibility for any injury to people or property resulting from any ideas, methods, instructions or products referred to in the content.